Chemical Science

ROYAL SOCIETY OF CHEMISTRY

EDGE ARTICLE

View Article Online
View Journal | View Issue

Cite this: *Chem. Sci.*, 2021, **12**, 13809

All publication charges for this article have been paid for by the Royal Society of Chemistry

New Cy5 photosensitizers for cancer phototherapy: a low singlet–triplet gap provides high quantum yield of singlet oxygen†

He Ma,[a] Saran Long,*[ab] Jianfang Cao,[c] Feng Xu,[a] Panwang Zhou,[d] Guang Zeng,[e] Xiao Zhou,[a] Chao Shi,[a] Wen Sun,[ab] Jianjun Du,[ab] Keli Han,[f] Jiangli Fan[ab] and Xiaojun Peng[ab]

Highly efficient triplet photosensitizers (PSs) have attracted increasing attention in cancer photodynamic therapy where photo-induced reactive oxygen species (ROSs, such as singlet oxygen) are produced *via* singlet–triplet intersystem crossing (ISC) of the excited photosensitizer to kill cancer cells. However, most PSs exhibit the fatal defect of a generally less-than-1% efficiency of ISC and low yield of ROSs, and this defect strongly impedes their clinical application. In the current work, a new strategy to enhance the ISC and high phototherapy efficiency has been developed, based on the molecular design of a thio-pentamethine cyanine dye (TCy5) as a photosensitizer. The introduction of an electron-withdrawing group at the *meso*-position of TCy5 could dramatically reduce the singlet–triplet energy gap (ΔE_{st}) value (from 0.63 eV to as low as 0.14 eV), speed up the ISC process (τ_{ISC} = 1.7 ps), prolong the lifetime of the triplet state (τ_T = 319 μs) and improve singlet oxygen ($^1O_2$) quantum yield to as high as 99%, a value much higher than those of most reported triplet PSs. Further *in vitro* and *in vivo* experiments have shown that TCy5-CHO, with its efficient $^1O_2$ generation and good biocompatibility, causes an intense tumor ablation in mice. This provides a new strategy for designing ideal PSs for cancer photo-therapy.

Received 18th August 2021
Accepted 21st September 2021

DOI: 10.1039/d1sc04570a

rsc.li/chemical-science

Introduction

Various classes of chromophores are potential candidate triplet photosensitizers (PSs) that have been used in a wide range of applications such as photodynamic therapy (PDT),[1] photocatalysis,[2] triplet–triplet-annihilation upconversion,[3] and photovoltaics.[4] After being excited by light of a specific wavelength, the triplet PS reaches the excited state. Unlike the short-lived singlet state, the life span of the triplet state can reach microseconds or even milliseconds.[1d,5] The long lifetime of the T_1 state ensures the conversion of light energy to chemical energy, for example, for initiation of efficient intermolecular energy transfer to generate singlet oxygen or application in photovoltaics and photocatalysis *via* electron transfer. Generally, triplets are of lower energy than singlets based on Hund's rule of maximum multiplicity. Therefore, the electron can reach the triplet state from the excited singlet state *via* intersystem crossing (ISC),[6] whose efficiency determines the quantum yield of T_1. Thus, the efficiency of the ISC is the key feature of triplet PSs.

Substantial efforts have been devoted to enhancing the ISC of chromophores. One of the general strategies in this regard involves incorporating heavy atoms such as heavy halogen atoms (Br and I) and transition metals into the chromophore core.[7] Heavy atoms can help achieve efficient ISC by enhancing spin–orbit coupling (SOC).[5b,8] This heavy-atom strategy, while having led to the development of numerous triplet PSs, is still not applicable in many cases because the enhanced SOC also accelerates the transition from T_1 to S_0.[9] Also, heavy atom substitution always results in higher dark toxicity, which limits their biological applications.[10] To date, cyclic tetrapyrroles,[11] methylene blue,[12] and phenalenone[13] have been recognized as heavy-atom-free PSs. To systematically develop new PSs, several tailor-made strategies have been developed to produce heavy-atom-free PSs displaying efficient ISC. For instance, thionation of the carbonyl group in a chromophore is a new approach to reduce the energy gap between the S_n and T_m states, leading to efficient transition to the triplet state.[14] However, the various

[a]State Key Laboratory of Fine Chemicals, Dalian University of Technology, Dalian 116024, China. E-mail: srlong@dlut.edu.cn

[b]State Key Laboratory of Fine Chemicals and Shenzhen Research Institute, Dalian University of Technology, Dalian 116024, China

[c]School of Chemical Engineering, Dalian University of Technology, Panjin Campus, Panjin 124221, China

[d]Institute of Molecular Sciences and Engineering, Institute of Frontier and Interdisciplinary Science, Shandong University, Qingdao 266237, China

[e]State Key Laboratory of Catalysis, Dalian Institute of Chemical and Physics, Chinese Academy of Sciences, Zhongshan Road 457, Dalian 116023, China

[f]State Key Laboratory of Molecular Reaction Dynamics, Dalian Institute of Chemical Physics, Chinese Academy of Sciences, 457, Zhongshan Road, Dalian 116023, China

† Electronic supplementary information (ESI) available. See DOI: 10.1039/d1sc04570a

reactive oxygen species (ROSs) produced by PSs or other oxides perform single-atom sulfur-for-oxygen replacements, which bring about the inactivation of the PSs, implying that these PSs are not stable under light and cannot be reused.[15] Twisted π-conjugation systems[16] and orthogonal compact electron donor–acceptor dyads[17] have also been used to facilitate the ISC process, which also lead to relatively short absorption wavelengths. Based on the aggregation-induced emission (AIE) skeleton, the D–π–A strategy has been proven to be an efficient way to enhance ISC for AIE PS construction.[18] Recently, the Zhao group showed that a nearby free radical can transform the electronic configuration of a chromophore so that the ISC becomes a spin-allowed transition, which also helps enhance the ISC.[19] The instability of free radicals as an ineluctable drawback should not be ignored. Although these aforementioned insightful patterns have introduced new ideas for enhancing the ISC of PSs, developing a PS that displays both efficient ISC and other desired properties, *e.g.*, concise chemical construction, near infrared (NIR) light activation, and good water solubility, is still a challenge.

Reducing the singlet–triplet energy gap (ΔE_{st}) is another mechanism considered to be crucial in promoting the ISC.[20] Subsequently, the low ΔE_{st} of the PS will ensure high singlet oxygen ($^1O_2$) quantum yield (QY) which is a central element for treatment efficiency.[21] Despite this discovery providing an opportunity for developing novel heavy-atom-free PSs, the practice of this concept hitherto has managed to determine how to realize appropriate molecular designs. In the current work, we developed a new PS design strategy by introducing an electron-withdrawing group (EWG) at the *meso*-position of the thio-pentamethine cyanine dye (TCy5) to realize a reduction of ΔE_{st} and achieve an ISC enhancement (Fig. 1a). The ISC efficiency of the dye increased with the introduction of more strongly electron-withdrawing substituents. This molecular design strategy was indicated to be generally applicable to TCy5 scaffolds. As a result, TCy5 modified with a quaternary ammonium salt of benzothiazole (Btz) demonstrated an improved $^1O_2$ QY, up to 99%—and hence, to the best of our knowledge, performed better as an $^1O_2$ generator than has any previously reported PS. To further demonstrate the application of the PSs, TCy5-CHO was selected for PDT because of its efficient $^1O_2$ generation and good photostability. It showed powerful suppression of tumor cell proliferation and promising tumor therapy *in vivo*. This result showed TCy5-CHO to be an ideal heavy-atom-free PS, and hence indicated the promise of applying the triplet PS design strategy to a wider range of fields.

Results and discussion

Compared to the aforementioned triplet PS design strategy, systematic chemical modification of the chromophores may lead to tunable properties of the ΔE_{st}, as well as subsequent improvement of ISC performance. Because of their excellent properties, such as NIR absorption, good water solubility and tailorable structures, cyanine dyes were chosen initially. Herein, we synthesized a series of designed TCy5 derivative compounds and studied their production capacity for ROSs. As illustrated in Fig. 1a, both the ISC and fluorescence originated from S_1 and there is a general rule for designing triplet PSs: decreasing the ΔE_{st} value can enable the ISC to compete with the other process. Following the rule, we established a series of new triplet PSs by altering the *meso*-substituents (X) appended to TCy5 (Fig. 1b). In the beginning, we selected a generally used NIR absorbing chromophore, TCy5-H, which possessed intense absorption in the NIR region (λ_{abs} = 669 nm, $\varepsilon = 1.92 \times 10^5$ M^{-1} cm^{-1}) and a high fluorescence quantum yield (Φ_F = 56%) (Table 1).

Effect of substitution at the *meso*-position of TCy5

The succinct and versatile chemistry of TCy5 made it possible for us to carry out a rapid divergent synthesis of a series of TCy5 PSs. By performing the Knoevenagel condensation reaction, a group of new TCy5 compounds (TCy5-H, TCy5-Ph-MeO, TCy5-Ph-NO_2, TCy5-CHO and TCy5-Btz) with various kinds of group (X) appended to (substituted into) the TCy5 core were synthesized and characterized (Schemes S1–S3†). Compared to the

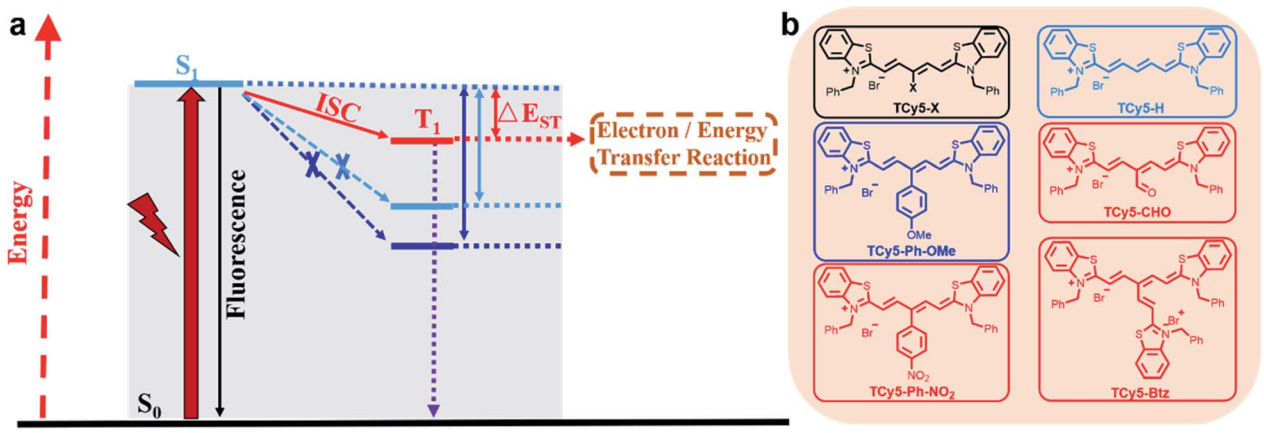

Fig. 1 (a) Schematic illustration of the strategy for our NIR excited TCy5 system *via* the optimization of the singlet–triplet energy gap (ΔE_{st}) by a *meso*-substitution group (X). (b) Molecular structures of the photosensitizers (TCy5-H, TCy5-Ph-MeO, TCy5-Ph-NO_2, TCy5-CHO and TCy5-Btz) in this study.

Table 1 Photophysical and photosensitizing properties of TCy5 compounds

	λ_{abs}/nm ($\varepsilon \times 10^{-3}$ M^{-1} cm^{-1})		λ_{em}/nm		Φ_F[c] (%)		
Compounds	DCM[a]	Water[b]	DCM[a]	Water[b]	DCM	Water	Φ_Δ[d] (%)
TCy5-H	669 (191.6)	654 (55.6)	690	675	56	11	0
TCy5-Ph-OMe	673 (95.2)	656 (31.1)	697	676	64	5	0
TCy5-Ph-NO_2	664 (120.1)	650 (60.6)	684	672	23	0.5	0
TCy5-CHO	627 (116.4)	591 (57.9)	665	644	21	2	63
TCy5-Btz	649 (52.8)	630 (33.5)	673	660	4	0.6	99

[a] In dichloromethane (DCM) with a concentration of 2 μM. [b] In ultrapure water (UW) with a concentration of 4 μM. [c] Absolute fluorescence quantum yield (Φ_F) upon irradiation at the corresponding absorption maxima. [d] Singlet oxygen quantum yield (Φ_Δ) is determined using Rose Bengal (RB) for TCy5 (Φ_Δ(RB) = 0.75 in water).

peak absorption and fluorescence wavelengths of TCy5-H, these wavelengths were found to be red-shifted when electron-donating groups (EDGs) were substituted into the core of TCy5-H and blue-shifted when electron-withdrawing groups (EWGs) were substituted into the core. The blue shift was attributed to the electron-deficient nature of X at the *meso*-position of the TCy5 moiety. The various TCy5 compounds strongly absorbed UV-visible light over a wide wavelength range, from as low as about 500 nm to as high as about 730 nm (Fig. 2a), *i.e.*, overlapping with the "therapeutic window" of 600–900 nm. In comparison with the organic phase, the five compounds also exhibited good solubility in ultrapure water (UW), important for their biological application prospects (Fig. S1a†). Their broad absorptions and high molar extinction coefficients suggested their strong light-harvesting abilities, a feature beneficial for PDT.

The fluorescence quantum yield (Φ_F) values for TCy5-H, TCy5-Ph-MeO, TCy5-Ph-NO_2, TCy5-CHO and TCy5-Btz in DCM were determined to be 56%, 64%, 23%, 21%, and 4%, respectively (Fig. 2b and Table 1). The high Φ_F of the initial compound TCy5-H demonstrated that it mainly underwent a radiative de-excitation. The even higher Φ_F observed when the electron-donating group 4-methoxybenzene was substituted into the *meso*-position of TCy5-H to produce TCy5-Ph-OMe illustrated that the electron-donating group might have strengthened the radiative process. The decrease of Φ_F (in DCM) to 23% when X was changed to the electron-deficient Ph-NO_2 was expected. And as shown above, when the aldehyde group was introduced at the *meso*-position of TCy5, the fluorescence quenching was much more obvious, and the powerfully electron-withdrawing quaternary ammonium salt yielded the strongest fluorescence quenching (Φ_F = 4% in DCM). The Φ_F in the aqueous phase also confirmed that the EWG could cut down radiative transition. Therefore, we ascribed the decreased Φ_F to the EWG at the *meso*-position. For each of the TCy5-EWG compounds, the wavelength of the center of the residual fluorescence in solution was shorter than that for reference compound TCy5-H (Table 1). This blue-shifted fluorescence emission was an indication of the orderly tunable conjugation between the TCy5 core and *meso*-substituted moiety. Compared with that of TCy5-H, the reduced fluorescence lifetime of TCy5-EWG was quite consistent with the fluorescence quantum yield measurements (Fig. S2 and Table S1†). These results showed a marked dependence of the reduction in the radiative process efficiency on having an EWG at the *meso*-position of the TCy5. The implication would be a promising indication of the availability of another efficient nonradiative decay channel for the S_1 state of each of the TCy5-EWG compounds, with ISC being one of the probable relaxation channels.

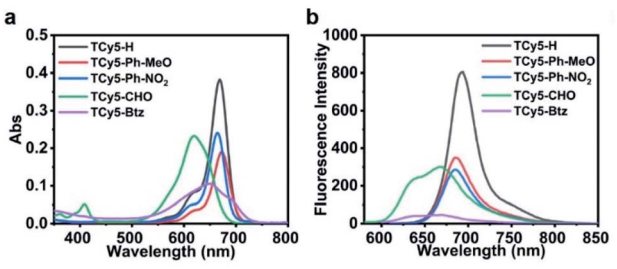

Fig. 2 (a) Absorption and (b) fluorescence of TCy5 compounds (2 μM) in DCM. Slit = 5/5.

$^1O_2$ detection and PDT efficiency

To better understand the distinct fluorescence quenching effects of the EWGs, molecular oxygen activation by the samples in water under NIR light irradiation was investigated. In our preliminary experiments, all TCy5 units having an EWG in the *meso*-position showed very high activity toward $^3O_2$, supporting the key role of EWGs in the ROS generation (Fig. 3). It has been shown that triplet photosensitizers for $^1O_2$ generation can be probed using 9,10-anthracenediylbis(methylene)dimalonic acid (ABDA), which selectively reacts with $^1O_2$, resulting in a decrease in ABDA absorbance.[22] In our experiments, aqueous solutions containing ABDA and the various TCy5 compounds, respectively, were exposed to NIR light, and the extent of any decrease in the concentration of ABDA was measured. A negligible decrease was observed for TCy5-H and for TCy5-Ph-OMe, demonstrating their negligible $^1O_2$ production capacities (Fig. 3c and S3†). Meanwhile, when TCy5-Ph-NO_2 was tested, a slight decrease in the concentration of ABDA was observed; this decrease indicated some enhancement of $^1O_2$ generation as a result of introducing the EWG. The intensity of the characteristic absorbance of ABDA showed a sustained decrease with time when testing TCy5-CHO as well as when testing TCy5-Btz

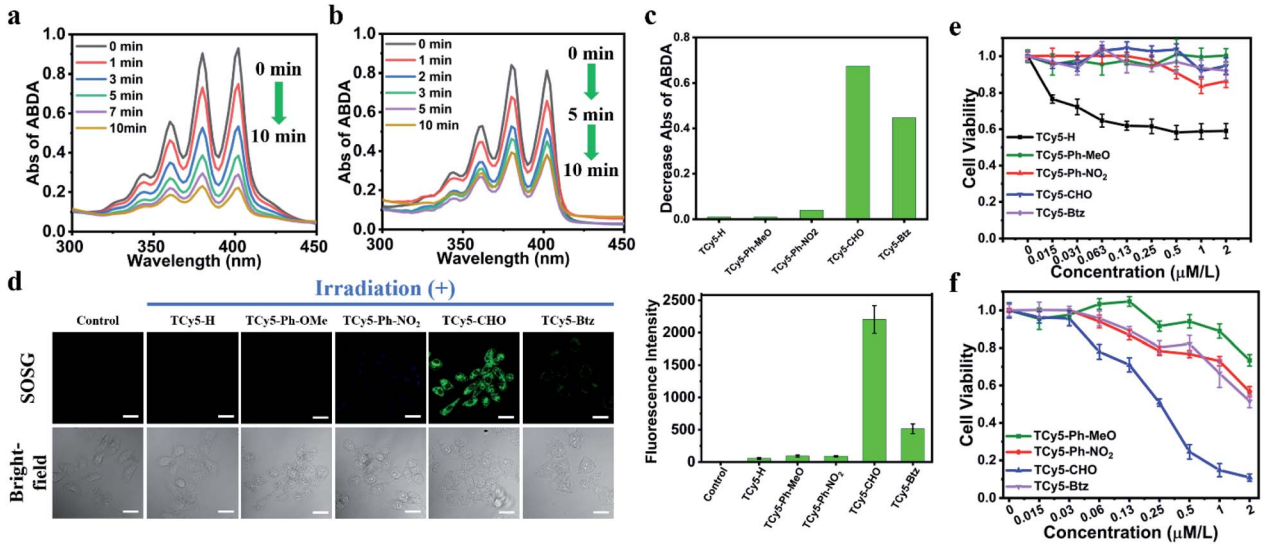

Fig. 3 Time-dependent UV-vis absorption spectra for 9,10-anthracenediyl-bis(methylene)-dimalonic acid (ABDA) over (a) TCy5-CHO and (b) TCy5-Btz under 10 mW cm^{-2} LED light irradiation in ultrapure water. (c) Decrease in the absorbance value of ABDA at 380 nm under NIR LED irradiation. (d) Fluorescence images of MCF7 cells containing TCy5 (5 μM)/SOSG (10 μM), indicating the $^1O_2$ generation of TCy5 dyes upon 660 nm light irradiation with a 20 J cm^{-2} light dose; for SOSG, emissions are collected at 500–580 nm (λ_{ex} = 488 nm). Scale bar = 20 μm. (e) Dark toxicity effect of TCy5 compounds on MCF7 cells. (f) Phototoxicity effect of four TCy5 compounds on MCF7 cells under 10 mW cm^{-2} light irradiation for 10 min.

(Fig. 3a and b), suggesting efficient production of $^1O_2$ in each case. The $^1O_2$ quantum yield (Φ_Δ) values of TCy5-CHO and TCy5-Btz were calculated to be 63% and 99%, respectively, using 1 mW cm^{-2} NIR light and Rose Bengal (RB) as the standard (Φ_Δ = 75% in water) (Fig. S4†). A comparison of our results with the literature showed these Φ_Δ values to be higher than the Φ_Δ values of most photosensitizers reported to date. The presence of $^1O_2$ was then tested for again using electron paramagnetic resonance (EPR) spectroscopy (Fig. S5†). The results of this experiment indeed suggested that $^1O_2$ was the predominant species, reflecting the energy transfer behavior in TCy5-CHO and TCy5-Btz. Of all the TCy5 samples investigated, TCy5-Btz was unusual in that it suddenly lost its efficacy within five minutes—with the nearly complete photobleaching in that short time frame undermining its further application (Fig. 3b and S6†). In contrast, the comparatively good photostability of TCy5-CHO ensured its ability to consistently generate a high amount of $^1O_2$ (Fig. 3a).[23]

To understand the striking difference between the rate of photobleaching of TCy5-CHO and that of TCy5-Btz, their cyclic voltammograms were acquired (Fig. S7 and Table S2†). Compared to TCy5-CHO, TCy5-Btz presented a lower irreversible oxidation potential, of 0.77 V, which might have been one of the reasons for its sharp photobleaching.

Encouraged by these promising results, we set out to determine the intracellular characteristics of these TCy5 dyes, specifically in MCF7 cells, and did so by using confocal laser-scanning microscopy (CLSM). Furthermore, we tested and compared the intracellular $^1O_2$ generation abilities of these TCy5 compounds by using the specific $^1O_2$ probe Singlet Oxygen Sensor Green (SOSG) (Fig. 3d). When subjected to 660 nm-wavelength irradiation, only the TCy5-CHO-treated MCF7 cells displayed obvious green fluorescence. TCy5-Btz showed only limited activation of SOSG, attributed to the above-described instability of TCy5-Btz upon being irradiated; and only relatively dim green fluorescence signals were observed in TCy5-H-, TCy5-Ph-MeO-, and TCy5-Ph-NO_2-treated cells, primarily due to their limited ISC capacities. These results revealed the superiority of TCy5-CHO, over the other TCy5 compounds, at promoting $^1O_2$ generation.

In light of the above promising results in cells, the potential of the TCy5 compounds to act as PDT agents was determined by using the MCF7 cells. Their levels of cytotoxicity in the dark and upon being exposed to light were investigated by using the methyl thiazolyl tetrazolium (MTT) assay for quantitative evaluation of cell viability. All TCy5 compounds were investigated with equal doses of light irradiated onto the different types of cell. In principle, an ideal PDT PS should be essentially nontoxic in the dark and highly toxic upon being exposed to light. Promisingly, TCy5-Ph-MeO, TCy5-Ph-NO_2, TCy5-CHO, and TCy5-Btz were found to be noncytotoxic in the dark in the MCF7 cells, while TCy5-H showed a cytotoxic profile in the range from 0.03 to 2 μM (Fig. 3e). When irradiated with 660 nm-wavelength light (10 min, 10 mW cm^{-2}), TCy5-Ph-MeO, TCy5-Ph-NO_2, and TCy5-Btz each showed little toxicity, with a half-maximal inhibitory concentration (IC_{50}) of greater than 2 μM (Fig. 3f). In contrast, TCy5-CHO showed notable phototoxicity upon being irradiated with light, with an IC_{50} value of only 0.25 μM.

Theoretical calculations and transition absorption measurements

To better understand the relationship between the chemical modifications of the TCy5 framework and the resulting ROS

generation, we performed time-dependent density functional theory (TD-DFT) investigations on the singlet and triplet excited states of the various TCy5 molecules. Their ground state geometries were optimized at the B3LYP/6-31+G(d, p) level of density functional theory (DFT). As shown in Fig. 4a, the entire LOMO distribution was determined from the DFT calculations to be fixed at the TCy5 core, while a clear difference between the HOMO and LUMO distributions of TCy5-Btz was observed. Above all, the respective ΔE_{st} values of the tested TCy5 compounds ranged from 0.14 to 0.63 eV. Specifically comparing the ΔE_{st} values of TCy5-Ph-NO_2, TCy5-CHO and TCy5-Btz, measured to be 0.61 eV, 0.50 eV, and 0.14 eV, respectively, showed how equipping TCy5 with a powerful EWG at the *meso*-position can result in a relatively low ΔE_{st} and easy access to the triplet state; thus TCy5-Btz could efficiently produce ROSs. The trend observed here was in agreement with that for the Φ_Δ experimental results.

To characterize in detail the overall temporal and structural changes from the absorption to the emission geometry in the photoexcited sample, transient absorption (TA) spectra of the TCy5-CHO and TCy5-H compounds dissolved in DCM were acquired for various delay times.

The evolution of femtosecond TA (fs TA) spectra of TCy5-H and TCy5-CHO in air-saturated DCM is shown in Fig. S8a† and 4b, respectively. Upon being subjected to a pulsed laser excitation at 380 nm, TCy5-CHO showed a broad excited-state absorption (ESA) band in the wavelength range of 450–570 nm, and a ground-state bleach (GSB) band centered at 630 nm. With increasing delay time, the ESA peak underwent a red-shift from a wavelength of about 490 nm at 1 ps to 530 nm at 6.1 ps. Compared with the negligible ESA of TCy5-H (Fig. S8a†), the new intense ESA for TCy5-CHO was due to the introduction of the EWG.

The ESA band from TCy5-CHO intensified substantially within 6.1 ps. A rise and set of decays of the trace at 530 nm were observed, as shown in Fig. 4b. The rise of the transient species was characterized by a time constant of 1.7 ps, which indicated the emergence of a new excited state.

Nanosecond TA spectra for TCy5-CHO in deaerated DCM were recorded (Fig. 4c) to evaluate the kinetics of the triplet excited states of TCy5-CHO upon being subjected to pulsed laser excitation at 355 nm. Remarkably, the ESA band was still seen for a long time, up to microseconds. Based on the nanosecond TA evidence, the duration of the rise (1.7 ps), shown in Fig. 4b, was assigned to the ISC process, which is even faster than that of a heavy-atom-PS. The broad ESA band in the wavelength range 420−550 nm was as strong as the GSB band, indicative of an efficient ISC displayed by TCy5-CHO. In addition, the decay trace at a wavelength of 627 nm showed a single-component decay (Fig. 4d). The triplet-state lifetime constants for the TCy5-CHO sample in deaerated DCM were observed to be 319 μs, and belong to T_1. Furthermore, the phosphorescence spectrum of TCy5-CHO also verified the ISC process (Fig. S9†).

The energy diagram of TCy5-CHO is presented in Fig. 4e. After TCy5-CHO was excited with NIR light, it will reach S_1 from S_0. The subsequent ISC (1.7 ps) produced the T_1 state, which competed with directly recovering to the *trans* ground state through a radiative transition (1.2 ns). The subsequent long ground-state bleach (319 μs) produced the initial S_0. The long lifetime of the triplet state and fast ISC process are the most important characters for a triplet PS.

PDT mechanism and efficiency of TCy5-CHO in live cells

Given their cationic characters, specifically with their positively charged chromophores, we had further thought that TCy5-CHO should be able to specifically accumulate in the mitochondria. As shown in Fig. 5a, S10 and S11,† its specific accumulation in the mitochondria was observed at an incubation time of 1 h. Note that, in general, generation of $^1O_2$ would be expected to

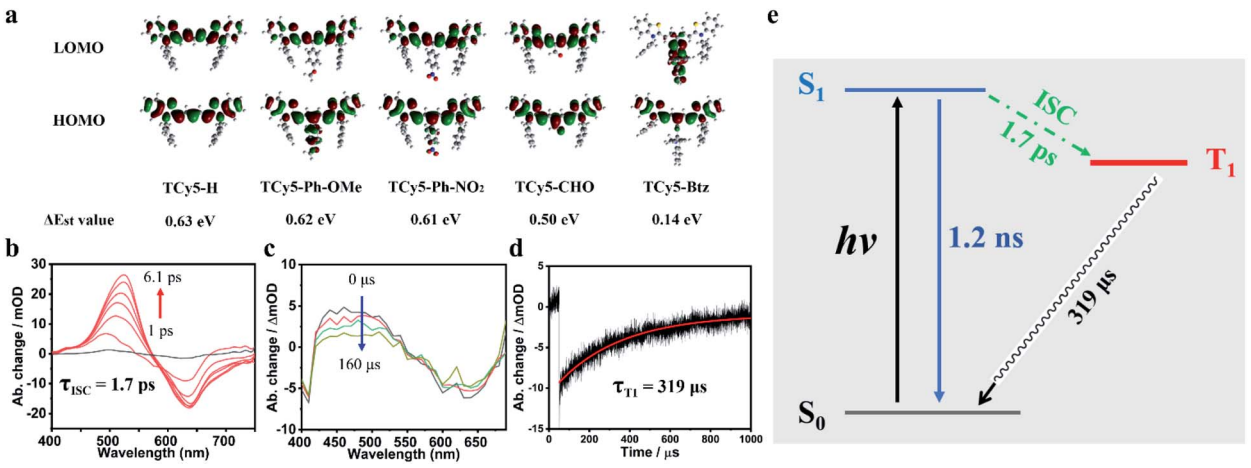

Fig. 4 (a) The HOMO–LUMO distribution of TCy5 is calculated by TD-DFT (Gaussian 09/B3LYP/6-31+G(d, p)). The ground state optimized geometry by the DFT calculations at the B3LYP/6-31G(d, p) level with Gaussian 09. (b) Femtosecond transient absorption spectra of TCy5-CHO, covering the time interval from 1 ps to 6.1 ps. (c) Nanosecond transient absorption spectra of TCy5-CHO excited with a nanosecond laser at 355 nm, and (d) decay trace at 627 nm of TCy5-CHO excited at 550 nm. $c = 3.0 \times 10^{-5}$ M in deaerated DCM at room temperature. Lifetimes of the single exponential fitting functions are given in the graph. (e) Schematic reduction of the potential energy diagram to illustrate the origin of the photophysical processes involved in TCy5-CHO shown in (b)–(d).

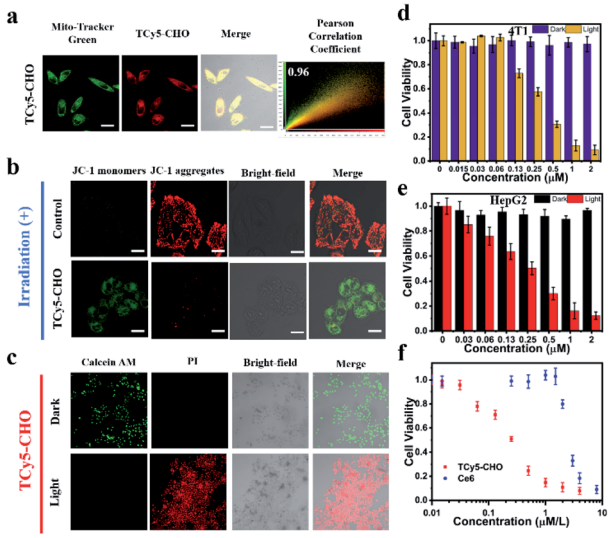

Fig. 5 (a) Representative confocal colocalization images of mitochondria (stained with MitoTracker Green) in MCF7 cells treated with compound TCy5-CHO (5 μM) for 1 h. For MitoTracker Green and TCy5, emissions were collected at 500–580 nm (λ_{ex} = 488 nm) and 650–730 nm (λ_{ex} = 640 nm), respectively. Scale bar = 20 μm. (b) Evaluation of mitochondrial membrane potential using probe JC-1 in MCF7 cells treated with compound TCy5-CHO and irradiated by 660 nm light with a 2 J cm^{-2} light dose. For JC-1, emissions are collected at 500–550 nm (λ_{ex} = 488 nm) and 580–630 nm (λ_{ex} = 561 nm), respectively. Scale bar = 20 μm. (c) Evaluation of tumoricidal efficacy using calcein AM/propidium iodide (PI) probes in MCF7 cells treated with compound TCy5 and irradiated with 660 nm light at 2 J cm^{-2}. Cell viability of HepG2 (d) and 4T1 (e) cells subjected to a range of TCy5-CHO concentrations under 10 mW cm^{-2} light irradiation for 10 min. (f) PDT effect comparison of TCy5-CHO and commercial Ce6 in MCF7 cells.

induce cellular injury and hence disrupt the integrity of the mitochondria. In the current work, mitochondrial membrane potential ($\Delta\Psi_m$) was measured using a JC-1 assay kit, with this assay operating based on a direct proportionality between the red fluorescence of the J-aggregates and the value of $\Delta\Psi_m$, and hence a decline in $\Delta\Psi_m$ upon conversion of the J-aggregates to their monomeric forms (green fluorescence).[24] As shown in Fig. 5b, TCy5-CHO effected a considerable loss of $\Delta\Psi_m$ with a small dose of light, namely, the green fluorescence observed in the MCF7 cells increased, and the intensities of the red signals decreased, as TCy5-CHO was irradiated. After the MCF7 cells were co-stained with calcein AM and propidium iodide (PI), most cells were red-stained (dead) (Fig. 5c). These striking results provided additional support for the potential effectiveness of TCy5-CHO as an $^1O_2$ PS.

In light of the above promising results in cells, we set out to investigate more extensive application possibilities for TCy5-CHO, and did so by evaluating its phototoxic effect in mouse breast cancer cells (4T1) and human liver carcinoma cells (HepG2) (Fig. 5d and e). Strikingly, TCy5-CHO also generated a phototoxic effect in these two types of cell and did so with IC_{50} levels (0.25 μM) similar to those of each other. As shown in Fig. 5e, the therapeutic efficacy of TCy5-CHO was found to be superior to that of commercial photosensitizer Ce6 under irradiation.

In vivo tumor PDT

Due to the promising abilities of TCy5 compounds to induce tumor cell death, we next examined the effect of performing treatments with TCy5-CHO and TCy5-Btz *in vivo*. After carrying out two-hour *in situ* injections of PBS or TCy5 into 4T1-tumor-bearing mice, the tumors of these mice were irradiated with a xenon lamp light subjected to an optical filter (660 nm, 50 mW cm^{-2}). For the *in vivo* PDT treatment, these mice were randomly divided into six groups, with each group containing five mice: (A) a group of mice injected with the PBS control (PBS), (B) mice treated with 660 nm-wavelength light irradiation after being injected with PBS (PBS + L), (C) mice only injected *in situ* with TCy5-Btz (TCy5-Btz), (D) mice injected *in situ* with TCy5-Btz and then treated with light (TCy5-Btz + L), (E) mice only injected *in situ* with TCy5-CHO (TCy5-CHO), and (F) mice injected *in situ* with TCy5-CHO and then treated with light irradiation (TCy5-CHO + L). The PDT treatment was conducted 2 h after *in situ* injection, and the irradiation was performed with 660 nm-wavelength light of 50 mW cm^{-2} for 15 minutes (Fig. 6a). Following the treatment, the PDT effects were evaluated by monitoring the change in tumor volume (Fig. 6b), number of mice that survived (Fig. 6c) and weights of the mice (Fig. 6d) as well as by performing hematoxylin and eosin (H&E) staining of the tumor tissues (Fig. 6e). Almost no tumor growth inhibition or tumor tissue necrosis was observed in the group of mice subjected to irradiation only, *i.e.*, without the test compounds (group B), which showed that, by itself, the NIR light irradiation with the power intensity used had little photothermal effect on the tumors. Regarding groups C and E, injections of TCy5-Btz and TCy5-CHO without any subsequent light therapy resulted in each case in hardly any tumor inhibition, *i.e.*, there was negligible dark toxicity demonstrated. Regarding group D

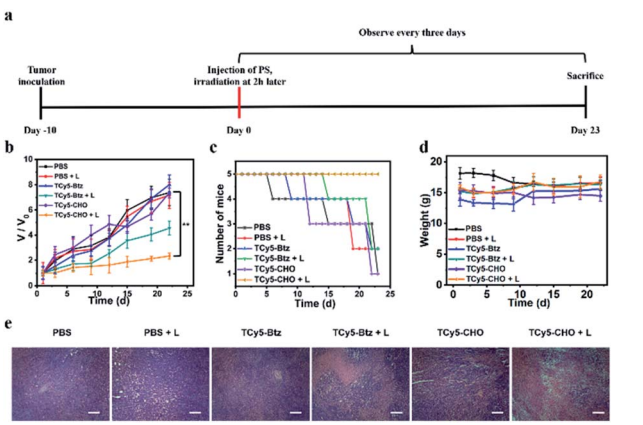

Fig. 6 (a) Schematic illustration of the *in vivo* photodynamic therapy by TCy5. (b) The changes of tumor volume of 4T1-tumor-bearing mice after different treatments: (A) PBS, (B) PBS + light (L) (660 nm, 50 mW cm^{-2}), (C) TCy5-Btz, (D) TCy5-Btz + L (660 nm, 50 mW cm^{-2}), (E) TCy5-CHO, (F) TCy5-CHO + L (660 nm, 50 mW cm^{-2}). Data are expressed as the mean and SD (n = 5 mice per group). (c) Survival line chart of different mice groups. (d) The body weight changes of mice receiving different treatments. (e) Typical images of H&E-stained tumors from mice that underwent different treatments for three days (scale bar = 100 μm). $^{**}p < 0.01$, $^{***}p < 0.001$.

(TCy5-Btz + L), injection of TCy5-Btz followed by irradiation also did not show an obvious therapeutic effect, which suggested the above-described photolability of TCy5-Btz still being an impediment to its application *in vivo*. In contrast, the tumor growth was markedly suppressed by the treatment involving injection of TCy5-CHO followed by irradiation: here, the tumor volume inhibition efficiency was found to be about 85%, and the survival rate was the highest of all of the groups (Fig. 6b and c).

The H&E staining analysis of the tumor tissue subjected to TCy5-CHO and light showed obvious necrosis, which indicated that TCy5-CHO can be effectively activated by NIR energy to generate ROSs, leading to an intensely phototoxic effect on the tumor (Fig. 6e). Additionally, neither cell necrosis nor inflammation lesions were detected in major organs such as the lungs, heart, liver, spleen and kidneys (Fig. S12†). These results suggested that TCy5-CHO displayed good biocompatibility and bioactivity *in vivo*.

Conclusions

We have demonstrated a new strategy for realizing an orderly decrease of singlet–triplet energy gaps (ΔE_{st}), by carrying out molecular modification and enhancing intersystem crossing (ISC) based on the heavy-atom-free TCy5. The introduction of an electron-withdrawing group (EWG) at the *meso*-position of TCy5 can make it become a triplet photosensitizer. Density functional theory calculations indicated a decreasing ΔE_{st}, from 0.63 eV to 0.14 eV, with increasing electron-withdrawing strength of the EWG. Induced by the EWG, the desired characters for a triplet PS, a fast ISC process (1.7 ps) and prolonged triplet state (319 μs), were achieved. This kind of triplet PS was concluded to exhibit an exceptional capability to generate singlet oxygen. In terms of application, TCy5-CHO was found to exhibit excellent phototoxicity against cancer cell proliferation by disrupting the integrity of mitochondria with a half-maximal inhibitory concentration (IC_{50}) of merely 0.25 μM under mild NIR light (10 mW cm^{-2}, 10 min). The high efficiency of TCy5-CHO was retained in different cell lines and was much higher than that of Ce6. Finally, we have demonstrated that using a powerful electron-withdrawing group as a substituent (X) might be a general strategy to develop efficient cyanine PSs. We plan in our following work to take advantage of this new strategy to further investigate triplet PSs.

Author contributions

H. M. and X. P. conceived the project. H. M., S. L., J. C., F. X., P. Z., X. Z., and C. S. performed the experiments. H. M., G. Z., W. S., J. D., K. H., J. F., and X. P. discussed the results. H. M. and X. P. wrote the manuscript.

Conflicts of interest

The authors declare no competing financial interest.

Acknowledgements

This work was supported by the National Natural Science Foundation of China (project 22090011) and NSFC-Liaoning United Fund (U1908202).

References

1 (*a*) D. E. J. G. J. Dolmans, D. Fukumura and R. K. Jain, *Nat. Rev. Cancer*, 2003, **3**, 380–387; (*b*) X. Li, S. Lee and J. Yoon, *Chem. Soc. Rev.*, 2018, **47**, 1174–1188; (*c*) J. P. Celli, B. Q. Spring, I. Rizvi, C. L. Evans, K. S. Samkoe, S. Verma, B. W. Pogue and T. Hasan, *Chem. Rev.*, 2010, **110**, 2795–2838; (*d*) V.-N. Nguyen, Y. Yan, J. Zhao and J. Yoon, *Acc. Chem. Res.*, 2021, **54**, 207–220; (*e*) H. Fan, G. Yan, Z. Zhao, X. Hu, W. Zhang, H. Liu, X. Fu, T. Fu, X.-B. Zhang and W. Tan, *Angew. Chem., Int. Ed.*, 2016, **55**, 5477–5482; (*f*) H.-W. Liu, X.-X. Hu, K. Li, Y. Liu, Q. Rong, L. Zhu, L. Yuan, F.-L. Qu, X.-B. Zhang and W. Tan, *Chem. Sci.*, 2017, **8**, 7689–7695; (*g*) Z. Yu, W. Pan, N. Li and B. Tang, *Chem. Sci.*, 2016, **7**, 4237–4244.

2 (*a*) D. Ravelli, M. Fagnoni and A. Albini, *Chem. Soc. Rev.*, 2013, **42**, 97–113; (*b*) J. Zhao, W. Wu, J. Sun and S. Guo, *Chem. Soc. Rev.*, 2013, **42**, 5323–5351; (*c*) L. Shi and W. Xia, *Chem. Soc. Rev.*, 2012, **41**, 7687–7697; (*d*) W. Wu, S. Xu, G. Qi, H. Zhu, F. Hu, Z. Liu, D. Zhang and B. Liu, *Angew. Chem., Int. Ed.*, 2019, **58**, 3062–3066; (*e*) T. Kim, S. J. McCarver, C. Lee and D. W. C. MacMillan, *Angew. Chem., Int. Ed.*, 2018, **57**, 3488–3492; (*f*) K. Koike, D. C. Grills, Y. Tamaki, E. Fujita, K. Okubo, Y. Yamazaki, M. Saigo, T. Mukuta, K. Onda and O. Ishitani, *Chem. Sci.*, 2018, **9**, 2961–2974; (*g*) J.-H. Shon, D. Kim, M. D. Rathnayake, S. Sittel, J. Weaver and T. S. Teets, *Chem. Sci.*, 2021, **12**, 4069–4078; (*h*) Y. Tamaki, K. Koike and O. Ishitani, *Chem. Sci.*, 2015, **6**, 7213–7221.

3 (*a*) T. N. Singh-Rachford and F. N. Castellano, *Acc. Chem. Res.*, 2010, **254**, 2560–2573; (*b*) L. Huang, W. Wu, Y. Li, K. Huang, L. Zeng, W. Lin and G. Han, *J. Am. Chem. Soc.*, 2020, **142**, 18460–18470; (*c*) J. Zhou, Q. Liu, W. Feng, Y. Sun and F. Li, *Chem. Rev.*, 2015, **115**, 395–465.

4 (*a*) T. F. Schulze and T. W. Schmidt, *Energy Environ. Sci.*, 2015, **8**, 103–125; (*b*) G. Yu, J. Gao, J. C. Hummelen, F. Wudl and A. J. Heeger, *Science*, 1995, **270**, 1789; (*c*) D. N. Congreve, J. Lee, N. J. Thompson, E. Hontz, S. R. Yost, P. D. Reusswig, M. E. Bahlke, S. Reineke, T. Van Voorhis and M. A. Baldo, *Science*, 2013, **340**, 334; (*d*) G. Han, T. Hu and Y. Yi, *Adv. Mater.*, 2020, **32**, 2000975.

5 (*a*) Y. You and W. Nam, *Chem. Soc. Rev.*, 2012, **41**, 7061–7084; (*b*) S. Monro, K. L. Colón, H. Yin, J. Roque, P. Konda, S. Gujar, R. P. Thummel, L. Lilge, C. G. Cameron and S. A. McFarland, *Chem. Rev.*, 2019, **119**, 797–828; (*c*) J. Zhao, K. Xu, W. Yang, Z. Wang and F. Zhong, *Chem. Soc. Rev.*, 2015, **44**, 8904–8939.

6 M. Kasha, *Discuss. Faraday Soc.*, 1950, **9**, 14–19.

7 (*a*) F. Xu, H. Li, Q. Yao, H. Ge, J. Fan, W. Sun, J. Wang and X. Peng, *Chem. Sci.*, 2019, **10**, 10586–10594; (*b*) J. Tian, J. Zhou, Z. Shen, L. Ding, J.-S. Yu and H. Ju, *Chem. Sci.*, 2015, **6**, 5969–5977; (*c*) S. Cetin, Z. Elmazoglu, O. Karaman,

H. Gunduz, G. Gunbas and S. Kolemen, *ACS Med. Chem. Lett.*, 2021, **12**, 752–757; (*d*) T. Almammadov, G. Atakan, O. Leylek, G. Ozcan, G. Gunbas and S. Kolemen, *ACS Med. Chem. Lett.*, 2020, **11**, 2491–2496.

8 (*a*) M. Lan, S. Zhao, W. Liu, C.-S. Lee, W. Zhang and P. Wang, *Adv. Healthcare Mater.*, 2019, **8**, 1900132; (*b*) T. Yogo, Y. Urano, Y. Ishitsuka, F. Maniwa and T. Nagano, *J. Am. Chem. Soc.*, 2005, **127**, 12162–12163; (*c*) D. P. Hari and B. König, *Chem. Commun.*, 2014, **50**, 6688–6699; (*d*) M.-K. Hung, K.-W. Tsai, S. Sharma, J.-Y. Wu and S.-A. Chen, *Angew. Chem., Int. Ed.*, 2019, **58**, 11317–11323.

9 (*a*) H. Uoyama, K. Goushi, K. Shizu, H. Nomura and C. Adachi, *Nature*, 2012, **492**, 234–238; (*b*) W. Zhang, J. Jin, Z. Huang, S. Zhuang and L. Wang, *Sci. Rep.*, 2016, **6**, 30178.

10 S. H. Lim, C. Thivierge, P. Nowak-Sliwinska, J. Han, H. van den Bergh, G. Wagnières, K. Burgess and H. B. Lee, *J. Med. Chem.*, 2010, **53**, 2865–2874.

11 (*a*) M. O. Senge and J. C. Brandt, *Photochem. Photobiol.*, 2011, **87**, 1240–1296; (*b*) J. J. Schuitmaker, E. W. Vogel, J. F. Nagelkerke and R. P. Bos, *J. Photochem. Photobiol., B*, 1998, **47**, 211–215; (*c*) B. Marydasan, R. R. Nair, P. S. S. Babu, D. Ramaiah and S. A. Nair, *ACS Omega*, 2019, **4**, 12808–12816; (*d*) J. Xia, M. Qian, Q. Yao, Z. Meng, H. Cui, L. Zhang, Y. Li, S. Wu, J. Wang, Q. Chen and X. Peng, *J. Controlled Release*, 2021, **334**, 263–274; (*e*) J. Xia, L. Zhang, M. Qian, Y. Bao, J. Wang and Y. Li, *J. Colloid Interface Sci.*, 2017, **498**, 170–181.

12 (*a*) Y. Yong, L. Zhou, Z. Gu, L. Yan, G. Tian, X. Zheng, X. Liu, X. Zhang, J. Shi, W. Cong, W. Yin and Y. Zhao, *Nanoscale*, 2014, **6**, 10394–10403; (*b*) M. Qin, H. J. Hah, G. Kim, G. Nie, Y.-E. K. Lee and R. Kopelman, *Photochem. Photobiol. Sci.*, 2011, **10**, 832–841; (*c*) X. He, X. Wu, K. Wang, B. Shi and L. Hai, *Biomaterials*, 2009, **30**, 5601–5609.

13 (*a*) E. M. Digby, O. Sadovski and A. A. Beharry, *Chem.–Eur. J.*, 2020, **26**, 2713–2718; (*b*) R. Schmidt, C. Tanielian, R. Dunsbach and C. Wolff, *J. Photochem. Photobiol., A*, 1994, **79**, 11–17; (*c*) M. L. Salmerón, J. Quintana-Aguiar, J. V. De La Rosa, F. López-Blanco, A. Castrillo, G. Gallardo and C. Tabraue, *Mol. Carcinog.*, 2018, **57**, 1525–1539; (*d*) K. R. Phatangare, S. K. Lanke and N. Sekar, *J. Fluoresc.*, 2014, **24**, 1827–1840.

14 V.-N. Nguyen, S. Qi, S. Kim, N. Kwon, G. Kim, Y. Yim, S. Park and J. Yoon, *J. Am. Chem. Soc.*, 2019, **141**, 16243–16248.

15 (*a*) J. Tang, M. A. Robichaux, K.-L. Wu, J. Pei, N. T. Nguyen, Y. Zhou, T. G. Wensel and H. Xiao, *J. Am. Chem. Soc.*, 2019, **141**, 14699–14706; (*b*) J. Tang, L. Wang, A. Loredo, C. Cole and H. Xiao, *Chem. Sci.*, 2020, **11**, 6701–6708; (*c*) V.-N. Nguyen, S. Heo, S. Kim, K. M. K. Swamy, J. Ha, S. Park and J. Yoon, *Sens. Actuators, B*, 2020, **317**, 128213.

16 (*a*) M. Sapir and E. V. Donckt, *Chem. Phys. Lett.*, 1975, **36**, 108–110; (*b*) K. Schmidt, S. Brovelli, V. Coropceanu, D. Beljonne, J. Cornil, C. Bazzini, T. Caronna, R. Tubino, F. Meinardi, Z. Shuai and J.-L. Brédas, *J. Phys. Chem. A*, 2007, **111**, 10490–10499; (*c*) K. Nagarajan, A. R. Mallia, K. Muraleedharan and M. Hariharan, *Chem. Sci.*, 2017, **8**, 1776–1782; (*d*) J. E. Norton and K. N. Houk, *J. Am. Chem. Soc.*, 2005, **127**, 4162–4163.

17 (*a*) M. A. Filatov, S. Karuthedath, P. M. Polestshuk, S. Callaghan, K. J. Flanagan, M. Telitchko, T. Wiesner, F. Laquai and M. O. Senge, *Phys. Chem. Chem. Phys.*, 2018, **20**, 8016–8031; (*b*) X.-F. Zhang, X. Yang and B. Xu, *Phys. Chem. Chem. Phys.*, 2017, **19**, 24792–24804; (*c*) D. J. Gibbons, A. Farawar, P. Mazzella, S. Leroy-Lhez and R. M. Williams, *Photochem. Photobiol. Sci.*, 2020, **19**, 136–158.

18 (*a*) W. Wu, D. Mao, F. Hu, S. Xu, C. Chen, C.-J. Zhang, X. Cheng, Y. Yuan, D. Ding, D. Kong and B. Liu, *Adv. Mater.*, 2017, **29**, 1700548; (*b*) S. Xu, Y. Yuan, X. Cai, C.-J. Zhang, F. Hu, J. Liang, G. Zhang, D. Zhang and B. Liu, *Chem. Sci.*, 2015, **6**, 5824–5830; (*c*) S. Wang, X. Wang, L. Yu and M. Sun, *Photodiagn. Photodyn. Ther.*, 2021, **34**, 102254; (*d*) D. Wang, M. M. S. Lee, G. Shan, R. T. K. Kwok, J. W. Y. Lam, H. Su, Y. Cai and B. Z. Tang, *Adv. Mater.*, 2018, **30**, 1802105.

19 Z. Wang, J. Zhao, A. Barbon, A. Toffoletti, Y. Liu, Y. An, L. Xu, A. Karatay, H. G. Yaglioglu, E. A. Yildiz and M. Hayvali, *J. Am. Chem. Soc.*, 2017, **139**, 7831–7842.

20 (*a*) X. Xiong, F. Song, J. Wang, Y. Zhang, Y. Xue, L. Sun, N. Jiang, P. Gao, L. Tian and X. Peng, *J. Am. Chem. Soc.*, 2014, **136**, 9590–9597; (*b*) V.-N. Nguyen, A. Kumar, M. H. Lee and J. Yoon, *Coord. Chem. Rev.*, 2020, **425**, 213545; (*c*) T. Li, D. Yang, L. Zhai, S. Wang, B. Zhao, N. Fu, L. Wang, Y. Tao and W. Huang, *Adv. Sci.*, 2017, **4**, 1600166; (*d*) Y.-L. Chen, S.-W. Li, Y. Chi, Y.-M. Cheng, S.-C. Pu, Y.-S. Yeh and P.-T. Chou, *ChemPhysChem*, 2005, **6**, 2012–2017; (*e*) V.-N. Nguyen, Y. Yim, S. Kim, B. Ryu, K. M. K. Swamy, G. Kim, N. Kwon, C. Y. Kim, S. Park and J. Yoon, *Angew. Chem., Int. Ed.*, 2020, **59**, 8957–8962.

21 (*a*) L. Huiyun, S. Yi, C. Defu, L. Lisheng, L. Buhong and X. Shusen, *Proc. SPIE*, 2010, **7845**, 78451j; (*b*) T. Montagnon, M. Tofi and G. Vassilikogiannakis, *Acc. Chem. Res.*, 2008, **41**, 1001–1011; (*c*) J. Ge, M. Lan, B. Zhou, W. Liu, L. Guo, H. Wang, Q. Jia, G. Niu, X. Huang, H. Zhou, X. Meng, P. Wang, C.-S. Lee, W. Zhang and X. Han, *Nat. Commun.*, 2014, **5**, 4596.

22 N. Adarsh, R. R. Avirah and D. Ramaiah, *Org. Lett.*, 2010, **12**, 5720–5723.

23 G. W. Byers, S. Gross and P. M. Henrichs, *Photochem. Photobiol.*, 1976, **23**, 37–43.

24 (*a*) L. Hao, Z.-W. Li, D.-Y. Zhang, L. He, W. Liu, J. Yang, C.-P. Tan, L.-N. Ji and Z.-W. Mao, *Chem. Sci.*, 2019, **10**, 1285–1293; (*b*) W. Zhou, X. Wang, M. Hu, C. Zhu and Z. Guo, *Chem. Sci.*, 2014, **5**, 2761–2770.